

RESEARCH

Ataxia-Telangiectasia Locus: Sequence Analysis of 184 kb of Human Genomic DNA Containing the Entire *ATM* Gene

Matthias Platzer,¹ Galit Rotman,² David Bauer,¹ Tamar Uziel,² Kinneret Savitsky,² Anat Bar-Shira,² Shlomit Gilad,² Yosef Shiloh,² and André Rosenthal^{1,3}

¹Department of Genome Analysis, Institute of Molecular Biotechnology, Jena 07745, Germany;

²Department of Human Genetics, Sackler School of Medicine, Tel Aviv University, Ramat Aviv 69978, Israel

Ataxia-telangiectasia (A-T) is an autosomal recessive disorder involving cerebellar degeneration, immunodeficiency, chromosomal instability, radiosensitivity, and cancer predisposition. The genomic organization of the A-T gene, designated *ATM*, was established recently. To date, more than 100 A-T-associated mutations have been reported in the *ATM* gene that do not support the existence of one or several mutational hotspots. To allow genotype/phenotype correlations it will be important to find additional *ATM* mutations. The nature and location of the mutations will also provide insights into the molecular processes that underly the disease. To facilitate the search for *ATM* mutations and to establish the basis for the identification of transcriptional regulatory elements, we have sequenced and report here 184,490 bp of genomic sequence from the human 11q22–23 chromosomal region containing the entire *ATM* gene, spanning 146 kb, and 10 kb of the 5'-region of an adjacent gene named *E14/NPAT*. The latter shares a bidirectional promoter with *ATM* and is transcribed in the opposite direction. The entire region is transcribed to ~85% and translated to 5%. Genome-wide repeats were found to constitute 37.2%, with LINE (17.1%) and *Alu* (14.6%) being the main repetitive elements. The high representation of LINE repeats is attributable to the presence of three full-length LINE-1s, inserted in the same orientation in introns 18 and 63 as well as downstream of the *ATM* gene. Homology searches suggest that *ATM* exon 2 could have derived from a mammalian interspersed repeat (MIR). Promoter recognition algorithms identified divergent promoter elements within the CpG island, which lies between the *ATM* and *E14/NPAT* genes, and provide evidence for a putative second *ATM* promoter located within intron 3, immediately upstream of the first coding exon. The low G + C level (38.1%) of the *ATM* locus is reflected in a strongly biased codon and amino acid usage of the gene.

[The sequence data described in this paper have been submitted to the GenBank data library under accession no. U82828.]

Ataxia telangiectasia (A-T) is an autosomal recessive disorder with a remarkable range of clinical manifestations affecting different tissues. It has a frequency of 1:40,000–100,000 live births worldwide. A-T patients suffer from progressive neurological degeneration, immune deficiency, lymphoreticular malignancies, chromosomal instability, growth retardation, gonadal dysgenesis, telangiectases (dilated blood vessels) appearing in the eyes and face, and premature aging of skin and hair (for review, see Shiloh 1995; Lavin and Shiloh 1997). Epidemiologi-

cal studies of A-T heterozygotes have suggested an elevated risk for cancer, particularly breast cancer (Swift et al. 1991). Cultured cells from these individuals show an increased sensitivity to ionizing radiation (Weeks et al. 1991).

The gene mutated in A-T patients (*ATM*) was mapped to chromosome 11q22–23 (Gatti et al. 1988) and has been identified recently by positional cloning (Savitsky et al. 1995a). It contains an open reading frame (ORF) of 9168 nucleotides. The predicted protein of 3056 amino acids belongs to a family of large proteins that share sequence homologies to the catalytic domain of phosphatidylinositol-3 (PI-3) kinases (Savitsky et al. 1995b). Among these proteins are TEL1p and MEC1p in

³Corresponding author.
E-MAIL arosenth@imb-jena.de; FAX 49-3641-656255.

SEQUENCE ANALYSIS OF HUMAN *ATM*

budding yeast, Rad3 in fission yeast, the TOR proteins in yeast and their mammalian counterpart, FRAP (RAFT1), mei-41 in *Drosophila melanogaster*, and the catalytic subunit of DNA-dependent protein kinase in mammals. These proteins are involved in signal transduction, meiotic recombination, and control of cell cycle (for review, see Savitsky et al. 1995b; Zakian et al. 1995).

More than 100 mutations have been identified so far among A-T patients and these are spread over the entire coding region of the *ATM* gene. The vast majority of the mutations are expected to inactivate the ATM protein by truncation or large deletions. Most of the patients were found to be compound heterozygotes (Baumer et al. 1996; Byrd et al. 1996a; Gilad et al. 1996; Telatar et al. 1996; Wright et al. 1996).

To enable screening of A-T mutations based on genomic DNA as the resource, we have determined previously the entire genomic organization of the *ATM* gene. It is composed of 66 exons spread over a genomic region of ~150 kb (Uziel et al. 1996). Other groups have confirmed our findings (Rasio et al. 1996; Vorechovsky 1996). Analysis of the promoter region and mapping of cDNAs to the *ATM* locus revealed a second gene, designated *E14* (Byrd et al. 1996a,b) or *NPAT* (nuclear protein mapped to the *AT*-locus; Imai et al. 1996), 0.5 kb upstream of *ATM*. The *E14/NPAT* gene is transcribed in the opposite direction and codes for a 1421-amino-acid protein. *ATM* and *E14/NPAT* are both ubiquitously expressed and probably regulated by a bidirectional promoter (Byrd et al. 1996b).

Because of the importance of the *ATM* gene in biomedical research, we carried out a large-scale sequencing effort of the entire *ATM* genomic locus. By sequencing five cosmids derived from a cosmid contig spanning most of the D11S384–D11S1818 interval (Savitsky et al. 1995b), we have determined a contiguous genomic stretch of 184,490 bp containing the entire *ATM* gene as well as the 5' region of the *E14/NPAT* gene. In addition, we have obtained a comprehensive map of repeated elements and predicted several putative promoters. One potential secondary promoter region is located within intron 3 of the *ATM* gene, immediately upstream of the first coding exon. Together with the recently determined 5' and 3' untranslated regions (UTRs), which

display large variability, these data suggest a complex posttranscriptional regulation of the *ATM* gene (Savitsky et al. 1997). The complete genomic sequence of the *ATM* gene is a valuable resource for detection of all A-T mutations and for carrier diagnostics. The sequence also provides new insights into the organization and the evolution of the *ATM* locus.

RESULTS

Genomic Sequencing of 184 kb Spanning the *ATM* Locus

A cosmid contig between chromosomal markers D11S384 and D11S535 spanning the coding region of the *ATM* gene (Savitsky et al. 1995b) served as the starting point for sequencing. Five cosmids, B10, A12, C7, C12, and E3 (Fig. 1), were completely sequenced using the M13 random shotgun method. A region of ~10 kb between cosmids A12 and C7 was bridged by PCR products generated from exons 24–27.

Sequencing revealed that four of the five cosmids (A12, C7, C12, E3) carry the *Escherichia coli* transposon *Tn1000* (5981 bp) (Broom et al. 1995) as a cloning artifact. In cosmids A12, C7, and C12 the transposon was located within the human insert, whereas in cosmid E3 it was inserted in the cosmid vector. In addition, a previously unknown composite transposon of 4447 bp was identified in the human insert of cosmid C12. It comprises two insertion elements *IS10*, together with an *E. coli* sequence derived from the 81.5–84.5 min region (V.M. Platzer, unpubl.). Examination of the insertion sites of the *Tn1000* and the composite transposon revealed 5- and 9-bp duplications of the host DNA, respectively. To confirm that these duplications were artifacts caused by the transposon insertions and to exclude the possibility of additional alterations in

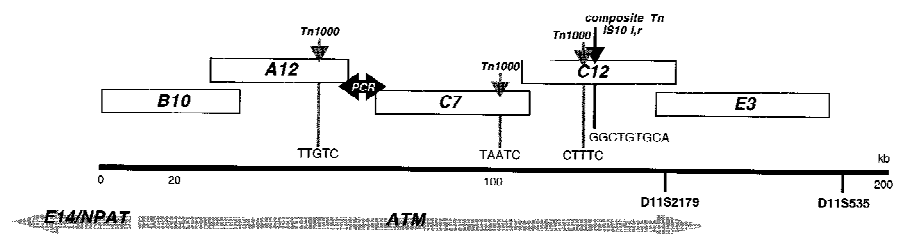


Figure 1 Cosmid contig across the sequenced region in 11q22–23. Horizontal arrows indicate orientation and coverage of *ATM* and *E14/NPAT* genes. Vertical arrows point to insertion sites of *E. coli* transposons, and the sequence of the duplications at the insertion sites are shown.

PLATZER ET AL.

the cosmid DNA, the integration sites were amplified from human genomic DNA (primers given in Table 1) and sequenced. No differences were found between the cosmid and genomic sequences except for the duplication of the insertion site.

The final genomic contig of 184,490 bp was derived from a total of 4659 sequencing reads with an average redundancy of 8.03 for the whole project. The sequence is completely double-stranded. We found that the use of dye-terminator chemistry in the shotgun phase significantly speeded up contig assembly and editing because it virtually eliminated compressions, frequently observed with dye-primers. Each position of the contig is represented by at least one dye-terminator read. The entire se-

quence was deposited in the GenBank database under accession no. U82828.

Recently, partial sequences of the *ATM* gene have been published (accession nos. U40887–U40918; Rasio et al. 1996; U55702–U55757; Vorechovsky et al. 1996) comprising 46,204 bp. GAP alignment of this data with the genomic contig of 184,490 bp revealed 188 discrepancies. After revision of the primary data, we were able to exclude errors at these positions in our sequence. Because many of the divergent positions in database entries U55702–U55757 are represented by N's or are found at the ends of the entries deep within introns, these data probably represent regions of poor quality rather than polymorphic sites. We also compared

Table 1. Exon–Intron Organization of the *ATM* gene

No.	Exon first base	Exon length	Intron first base	Intron length	No.	Exon first base	Exon length	Intron first base	Intron length
1a	10772	116	10888	184	33	80988	165	81153	1450
1b	11072	634	11706	89	34	82603	133	82736	2226
2	11795	43	11838	647	35	84962	96	85058	2330
3	12485	88	12573	2723	36	87388	172	87560	1761
4	15296	102	15398	77	37	89321	142	89463	1063
5	15475	113	15588	1289	38	90526	177	90703	1645
6	16877	146	17023	6344	39	92348	178	92526	3044
7	23367	165	23532	8107	40	95570	88	95658	2175
8	31639	166	31805	668	41	97833	156	97989	2095
9	32473	239	32712	1937	42	100084	88	100172	3321
10	34649	164	34813	1805	43	103493	89	103582	99
11	36618	170	36788	1595	44	103681	103	103784	1261
12	38383	372	38755	764	45	105045	149	105194	2430
13	39519	195	39714	785	46	107624	105	107729	1242
14	40499	96	40595	901	47	108971	120	109091	3887
15	41496	226	41722	2174	48	112978	235	113213	510
16	43896	126	44022	1140	49	113723	168	113891	1419
17	45162	126	45288	1379	50	115310	114	115424	1262
18	46667	90	46757	8094	51	116686	218	116904	975
19	54851	172	55023	1067	52	117879	208	118087	1022
20	56090	200	56290	2455	53	119109	114	119223	321
21	58745	83	58828	104	54	119544	159	119703	724
22	58932	156	59088	1125	55	120427	139	120566	985
23	60213	76	60289	114	56	121551	83	121634	999
24	60403	131	60534	6637	57	122633	141	122774	735
25	67171	118	67289	1386	58	123509	117	123626	7260
26	68675	174	68849	1540	59	130886	150	131036	2371
27	70389	170	70559	1347	60	133407	166	133573	1370
28	71906	247	72153	3123	61	134943	87	135030	6585
29	75276	116	75392	1262	62	141615	115	141730	936
30	76654	127	76781	498	63	142666	64	142730	10207
31	77279	200	77479	2815	64	152937	137	153074	106
32	80294	175	80469	519	65	153180	3774		

SEQUENCE ANALYSIS OF HUMAN *ATM*

the 184 kb genomic sequence with 4841 bp of the 5'-half of the *ATM* transcript (accession no. X91169; Byrd et al. 1996a) and with 2193 bp of the intergenic region between *ATM* and *E14/NPAT* (accession no. D83244; Imai et al. 1996). Although 14 discrepancies were detected, no sequencing errors within the primary data at the respective positions of our sequence could be identified. We therefore conclude, that at least 53,238 of the presented 184,490 bp were definitely obtained without any errors. This indicates an exceptional high sequencing accuracy for the database entry U82828.

Exon-Intron Structure of the *ATM* Gene with Single Base Pair Resolution

GAP alignment of the 184-kb sequence contig with the *ATM* mRNA containing the complete ORF (accession no. U33841; Savitsky et al. 1995b) and recently obtained cDNA clones representing alternative 5' and 3' ends of the *ATM* mRNA (accession nos. U67092 and U67093; Savitsky et al. 1997) revealed the exon-intron structure of the *ATM* gene at single base resolution. The *ATM* gene has 66 exons (Tab. 1; Fig. 2A). Donor and acceptor splice sites of the *ATM* gene follow the GT-AG consensus (Shapiro and Senapathy 1987). The only exception is the GC 5' splice site of intron 52. This GC variant is by far the most common nonconsensus mRNA splice site (Jackson 1991). It is the only alternative splice site known to allow accurate cleavage in vitro, although more slowly than the usual GT sequence (Aebi 1987). The genomic structure is consistent

with our previous results from cDNA sequencing and long-distance PCR using human DNA as the template (Uziel et al. 1996). It also proves the colinearity of the cosmid and genomic sequence.

The introns vary considerably in size from 77–10,207 bp. Homology search algorithms confirmed that the first exon of *E14/NPAT* (accession nos. D83243, U58852, and X97186) is located at a distance of 468 bp 5' of the first *ATM* exon, extending in the opposite orientation (Byrd et al. 1996a; Imai et al. 1996). We found no further match of the *E14/NPAT* mRNA sequence with the proximal 10,200 bp. This is consistent with the recently reported exon/intron structure of the gene (Byrd et al. 1996b), where intron 1 was reported to be >12 kb.

Using BLAST searches, we identified 20 expressed sequence tags (ESTs) that map to the *ATM* gene. The ESTs are highly redundant. Eighteen ESTs were from the 3590-bp long 3' UTR and of these, nine represent the extreme 3' end of the *ATM* mRNA. Only two ESTs (accession no. H43382 and H45943) were aligned to the coding region and mapped to the region of exons 62–65. Identical start points of both of these ESTs suggest that they were derived independently from the same cDNA clone.

We have used several gene prediction programs to predict exons in the 184-kb *ATM* locus. Their performance, however, was quite poor. Initially, XPOUND and XGRAIL 1.2 did not predict any of the *ATM* exons, whereas XGRAIL version 1.3 predicted 41 out of the 66 *ATM* exons almost correctly but falsely predicted another 28. This stands in contrast to our own experience (accession nos. U52111

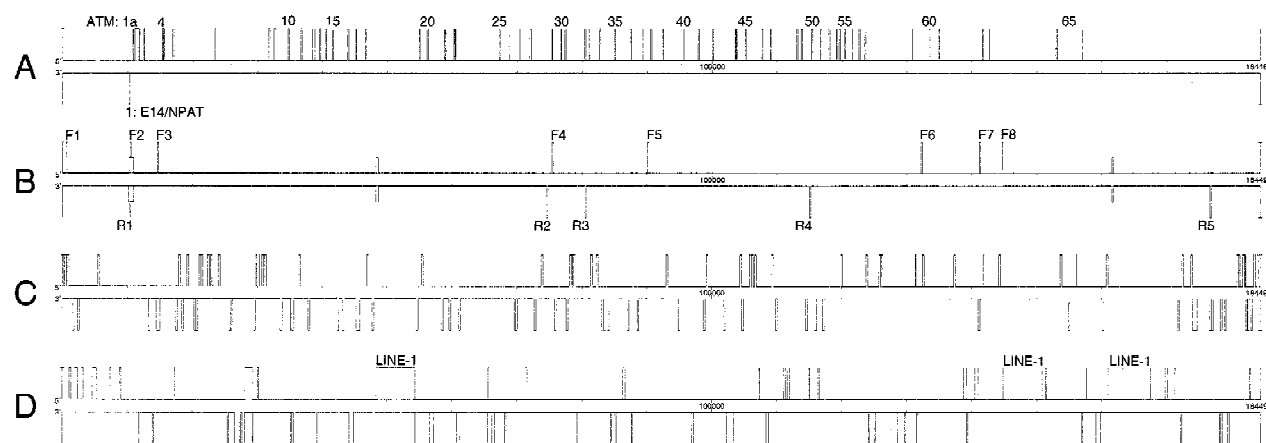


Figure 2 Schematic representation of the sequenced *ATM* locus. Boxes above the line represent features oriented toward the telomere; below the line, toward the centromere. (A) Exons identified by cDNAs. (B) CpG islands and predicted promoters (CpG islands are 0.5-high peaks; promoter regions are indicated by F and R in respect to their orientation). (C) SINEs. (D) LINEs, DNA transposons, and unclassified repeats.

PLATZER ET AL.

and U52112) and that of others (Lopez et al. 1994; Chen et al. 1996) who have noticed excellent performance of these programs in G + C-rich regions.

Repeat Analysis Reveals That *ATM* Exon 2 Is Related to a Genome-Wide Repetitive Element

Repeat analysis was performed to identify several types of simple-sequence repeats, microsatellites, and genome-wide repeats. Runs of five or more consecutive dinucleotides and trinucleotides are shown in Table 2. The dinucleotide repeat CA/TG was found at 12 sites in the region including marker D11S2179, 180 bp downstream to exon 62. Computer prediction revealed three copies of a 106-bp tandem repeat in intron 61, each repeat copy consisting of two head-to-tail arranged 53-bp units (position: 135,843; 136,024 and 136,209).

Genome-wide repeats were identified by CENSOR and divided into the four major classes (1) short interspersed nucleotide elements (SINE) [*Alu* and mammalian-wide interspersed repeats (MIRs)] (Smit and Riggs 1995; Batzer et al. 1996); (2) long interspersed nucleotide elements (LINEs) (Smit et al. 1995); (3) long terminal repeats [LTRs; and mammalian apparent LTR retrotransposons (MaLRs)] (Smit 1993); and (4) DNA transposons (Smit and Riggs 1996) (Table 3). Taken together, all genome-wide repeats together constitute 37.2% of the *ATM* locus, with *Alu* (14.6%) and LINE-1 (17.1%) being the major contributors (Fig. 2C,D).

Three full-length LINE-1s (6017, 6031, and 6116 bp) reside in introns 18 and 63, as well as 4.5 kb downstream of the polyadenylation site. They are oriented in the same direction as the *ATM* gene. Of the three LINE-1 repeats, only the two located in the

Table 2. Runs of More than Five Consecutive Dinucleotide and Trinucleotide Repeats

Sequence	Copies	Position	Localization	Rel. pos.
TA	5	5254	NPAT intron 1	+4947
TA	9	37828	ATM intron 11	-555
CA	5	38803	intron 12	+49
CA	5	56733	intron 20	+444
TG	7	58327	intron 20	-418
TG	6	62026	intron 24	+1493
TG	8	68202	intron 25	-473
TA	13	81568	intron 33	+416
TG	5	81594	intron 33	+442
TG	5	81620	intron 33	+468
TC	5	86981	intron 35	-407
TG	5	103030	intron 42	-463
TA	15	105288	intron 45	+95
CA	13	105318	intron 45	+125
TA	6	105345	intron 45	+152
TA	5	105385	intron 45	+192
GA	5	105422	intron 45	+229
TA	5	135887	intron 61	+858
TA	5	136070	intron 61	+1041
TA	5	136255	intron 61	+1226
CA	26	141909	intron 62	+180
TA	5	158201	ATM 3'	+1248
CA	6	159092	ATM 3'	+2139
TC	8	169782	ATM 3'	+12829
TG	9	178989	ATM 3'	+22036
CAA	6	330	NPAT intron 1	+9871
CAA	8	7439	NPAT intron 1	+2762
GAA	5	123978	ATM intron 58	+353
CAA	5	131465	intron 59	+430

Table 3. Distribution of Genome-Wide Repeats into the Main Four Classes of Human Transposable Elements

Type	Copies	Fraction of locus (%)
SINE		
<i>Alu</i>	103	14.6
MIR	12	1.1
LINE	36	17.1
LTR	—	—
DNA transposon	14	2.1
Unclassified	8	2.3
Total	173	37.2

introns are flanked by target-site duplications of 9 and 13 bp, respectively. The LINE-1s show more than 93% homology to LRE-1 (LINE-1 retransposable element; Dombroski et al. 1991); however, the presence of at least one premature termination codon in both LINE-1 ORFs suggests that none of them represents a transpositionally active element. A fourth LINE-1 repeat of 4212 bp was found in intron 24 in the opposite orientation. This repeat element is truncated at its 3'-end and shows only 74% homology to LRE-1.

All repeats, censored out using the initial conservative parameter set, are located deeply in the introns with the exception, that a MIR overlaps the intron 2 donor site (Fig. 3). The initial match obtained with CENSOR started at the last 3 bases of exon 2 and extended over a distance of 152 bp into intron 2 [score value 270 with $P(270)=3.4 \times 10^{-15}$]. This region is related to the 5' bases 12–165 of the 262-bp MIR consensus (Smit and Riggs 1995) and contains the entire box B and the 3' part of box A of the polymerase III promoter. Use of parameter settings at a higher sensitivity detected a similarity between the 3'-end of the MIR consensus and a region spanning 29 bp of the intron 1b acceptor site and the first 11 bp of exon 2 [score value 63 with $P(63)=0.0059$].

Local Content Analysis Reveals Large DNA Segments With Distinct G + C Content and a Major CpG Island in Between *ATM* and *E14/NPAT* Genes

Using a ± 2 -kb-window in steps of 1 kb, the G + C distribution along the 184 kb was estimated to be $38.1 \pm 2.9\%$ (mean \pm standard deviation).

As shown in Figure 4, we found two large re-

gions fluctuating around distinct G + C average values (1) The central region from 16–136 kb: $37.0 \pm 2.3\%$ and (2) the 3' region from 136–184 kb: $40.2 \pm 2.4\%$. If all genome-wide repeats are removed from the 184-kb *ATM* locus, the G + C content of the remaining 115,767 bp is 34.0%. Moreover, we found that the intron length of the central region correlates moderately with the G + C content. Shorter introns exhibit a lower G + C content regardless of their repeat content (Fig. 5).

Screening for CpG islands (Gardiner and Frommer 1987) in the 184-kb sequence contig identified a major CpG island from positions 10,186 to 10,943 (61.6% G + C; 0.88 CpG observed/expected). The first exons of *ATM* and *E14/NPAT* are contained within this CpG island. A BLAST search of this region identified a sequence (accession no. Z66089; six mismatches) that was obtained during construction of a human CpG island library (Cross et al. 1994). Two smaller CpG regions, predicted from positions 48,327 to 48,693; (59.4% G + C; 1.04 CpG observed/expected) and from 161,545 to 161,761 (62.2%; 1.00 CpG observed/expected), fall into the 5' region of LINE-1s.

The *ATM* Gene Shows a Biased Codon and Amino Acid Usage

The *ATM* gene resides at an A + T-rich portion of the human genome that can be classified as an L1 isochore (Bernardi et al. 1985). The G + C content of the first, second, and third codon positions is 47.5%, 34.2%, and 34.8%, respectively. The *ATM* codon and amino acid usage were compared with the human average values (9465 genes, GenBank

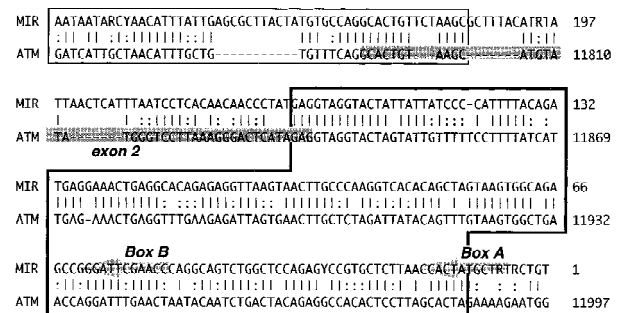


Figure 3 Sequence comparison of *ATM* exon 2 and the consensus of the genome-wide MIR repeat. Dark shaded regions indicate exons, lightly shaded arrows characteristic elements of the repeats, (Vbr) identities; (:) base transitions. Homology region with $P(270) = 3.4 \times 10^{-15}$ is located in the thick-lined box, the region with $P(65) = 0.0059$ in the thin-lined box.

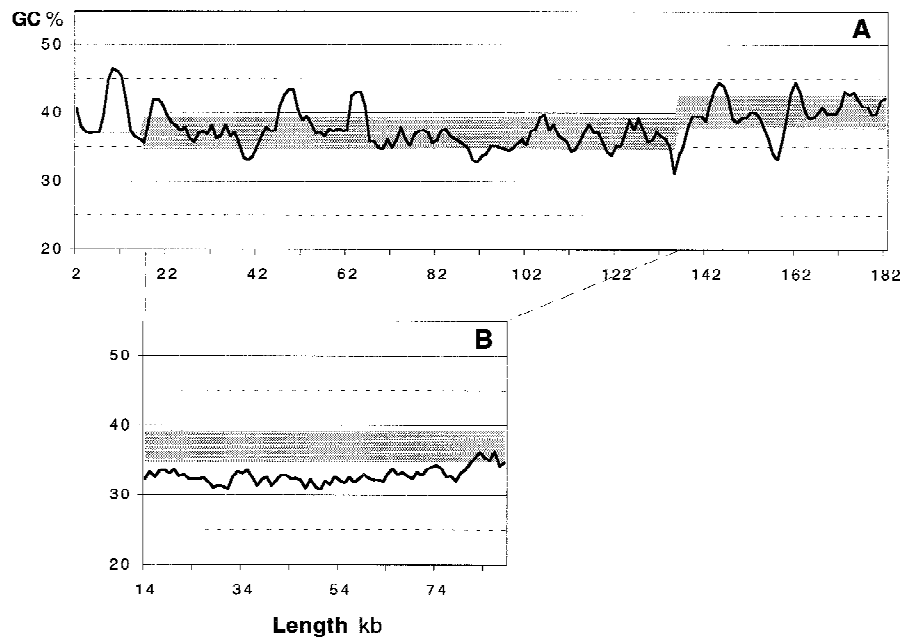


Figure 4 (A) G + C content of the sequenced *ATM* locus across the entire region 1–184 kb. Several distinct peaks above the G + C average represent genome-wide repeats (*Alu*: 61.38%; *LINE*: 41.73% G + C). (B) The region 14–136 kb relieved from genome-wide repeats. (A,B) Obtained with a moving window of ± 2 kb, step 1 kb.

release 96). Figure 6 shows a strong underrepresentation of codons with G or C in third position and of amino acids of the G/C class (i.e., amino acids with G and/or C in the first two codon positions: Arg, Ala, Gly, and Pro).

Promoter Prediction Reveals a Bidirectional Promoter in the CpG Island and Additional Promoter Elements for *ATM*

Two independent algorithms (TSSG/W, PSII) were used to identify potential promoter regions on both strands of the 184-kb sequence. Thirteen high-scoring promoter regions were predicted, eight in the direction of *ATM* transcription (F1–F8) and five in the direction of *E14/NPAT* (R1–R5) (Table 4; Fig. 2).

The promoter regions F2 and R1 are located within the CpG island covering the first exons of *ATM* and *E14/NPAT*, respectively. The intergenic region of 468 bp contains two CCAAT boxes and four SP1-binding sites (Byrd et al. 1996a,b). Several other regulatory elements were predicted, including three potential γ -interferon response elements (IREs; Yang et al. 1990).

The putative F3 promoter is of particular interest as it is located within intron 3 of the *ATM* gene,

just upstream of the first coding exon. The predicted promoter region overlaps with two *Alu* repeats. Interestingly, when the repetitive elements were removed from the analyzed region, the TSSG/W promoter prediction failed. One of the repeats, the *AluSg*, shows high homology to a functionally active *Alu* estrogen response element (ERE; Norris et al. 1995). The F3 putative promoter region contains potential binding sites for Sp1, AP1, AP2, CFI, GCF, and three TBP sites, one of which was identified as a TATA-box by TSSG/W (Fig. 7). Four additional putative promoter regions (F1, F5, F7, and R5) overlap with *Alu* repeats.

DISCUSSION

To gain further insight into the organization and function of the *ATM* gene, and to develop diagnostic reagents, we sequenced a cosmid contig spanning 184,490 bp containing the entire gene. With 66 exons, including the two alternatively spliced leader exons 1a and 1b, the *ATM* gene contains one of the largest number of exons reported to date for any human locus. The *ATM* exons are distributed over a genomic region of 146,182 bp. Therefore, the genomic organization of *ATM* is comparable with that of the Huntington disease gene with its 67 exons spread over 180 kb (Ambrose et al. 1994), but differs from that of giant genes such as *DMD* with 79 exons spread over 2.4 Mb (Roberts et al. 1993).

The human genome is a mosaic of long, compositionally homogeneous regions characterized by different G + C levels, called isochores. The G + C level of a genomic region has an impact on major genetic processes such as replication, transcription and recombination (for review, see Bernardi 1995). The 184-kb *ATM* contig shows a low G + C level of 38.1% and can be classified as part of a L1 isochore (Bernardi et al. 1985). This is consistent with the location of the *ATM* locus in the chromosomal region 11q22-23, a late-replicating G band that mainly consists of L1 and L2 isochores (for review, see Holmquist 1992). An analysis revealed a 3% shift in the local G + C average at position 136 kb between

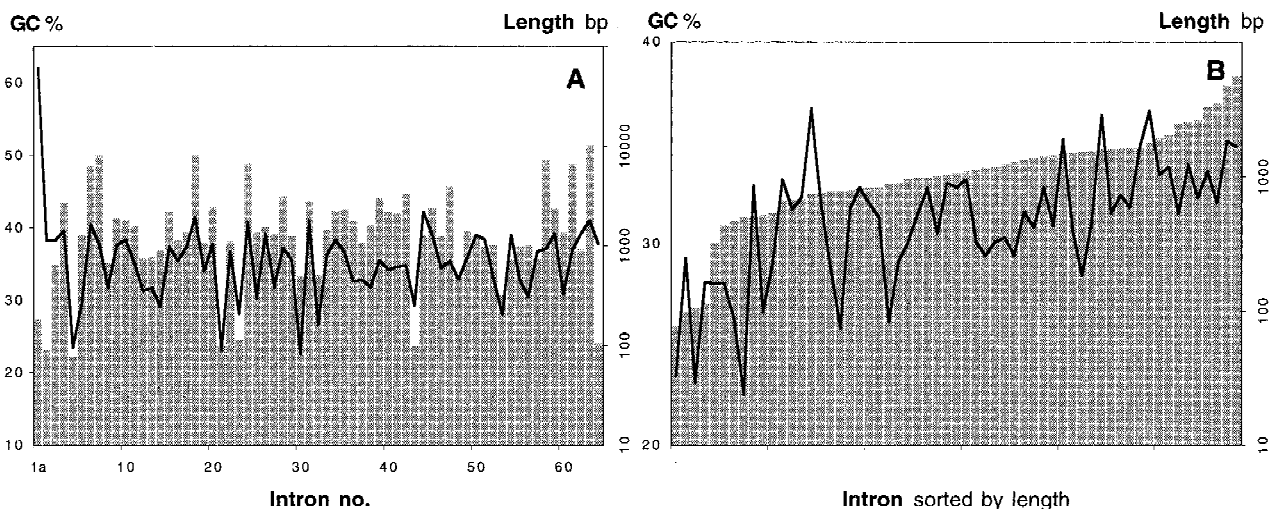
SEQUENCE ANALYSIS OF HUMAN *ATM*

Figure 5 Correlation of intron length and G + C content. (A) Introns sorted by number. (B) Introns 3–61 relieved from genome-wide repeats sorted by length. (Shaded bars) Intron length; (solid line) G + C content.

the proximal and the distal parts of the *ATM* gene and may represent an L1/L2 boundary. It is not as pronounced as the predicted isochore boundary between *G6PD* and *F8C* in human Xq28 (Ikemura et al. 1990) or the L/H and H2/H3 transitions in the human MHC locus of 6q21.3 (Fukagawa et al. 1995). The G + C shift separates the main body of the *ATM* gene from the 3' end where the predicted PI-3 kinase activity resides (Savitsky et al. 1995b). This may suggest that these two parts of the gene evolved and/or exist under different compositional constraints.

A + T-rich genes coding for long proteins are presently underrepresented in the databases (Duret et al. 1995). Because of this fact we have experienced considerable difficulties in exon prediction within the *ATM* contig. Although we failed to predict any *ATM* exon with XGRAIL 1.2 and XPOUND, XGRAIL 1.3 finally predicted 41 exons, but on the expense of 28 false positives. Our data highlight a current problem of gene prediction in A + T-rich isochores.

A considerable portion of the *ATM* locus (37.2%) represents genome-wide repeats. Removal of all these repeats from the *ATM* locus resulted in a more uniform, lower level G + C profile. Therefore it can be assumed that an ancient precursor of the human *ATM* locus exhibited an even lower G + C content before mammalian repeat expansion. There are three full-length LINE-1s in introns 18 and 63, as well as 4.5 kb downstream of *ATM*. The LINE-1s are highly conserved among each other, arranged in the same orientation and may represent hotspots for

homologous recombination (Bollag et al. 1989). The number of mutations disrupting the ORFs 1 and 2 of the three LINE-1 repeats suggests that the *ATM* locus was first invaded by the downstream LINE-1 followed by the element residing in intron 63. The LINE-1 repeat in intron 18 is probably of most recent origin, as its ORF1 is only once truncated by a single G/T substitution.

An interesting evolutionary aspect of the *ATM* gene structure is the homology between exon 2, its adjacent intronic sequences, and the genome-wide MIR repeat. During evolution, a large gene like *ATM* most certainly underwent processes like exon shuffling, exon skipping or intron shifting. We hypothesize that a MIR repeat has transposed into the *ATM* gene early in mammalian evolution and was later adopted as exon 2. Part of the MIR repeat functions as exon 2 splice donor site without major changes. However, the exon sequence itself and the acceptor site of intron 1b diverge from the MIR consensus, probably to fulfil requirements of mRNA secondary structure and stability, as well as of the splicing process.

Scanning of the 184-kb contig for potential promoter sites by different computer algorithms revealed several high-scoring regions. Two divergent promoters were predicted within a CpG island (for reviews, see Gardiner and Frommer 1987; Cross and Bird 1995). The island spans the first exons of *ATM* and the adjacent *E14/NPAT* and the intergenic region of 468 bp (Byrd et al. 1996a; Imai et al. 1996). This compact arrangement of the *ATM* and *E14/NPAT* genes is surprising, because both genes are

PLATZER ET AL.

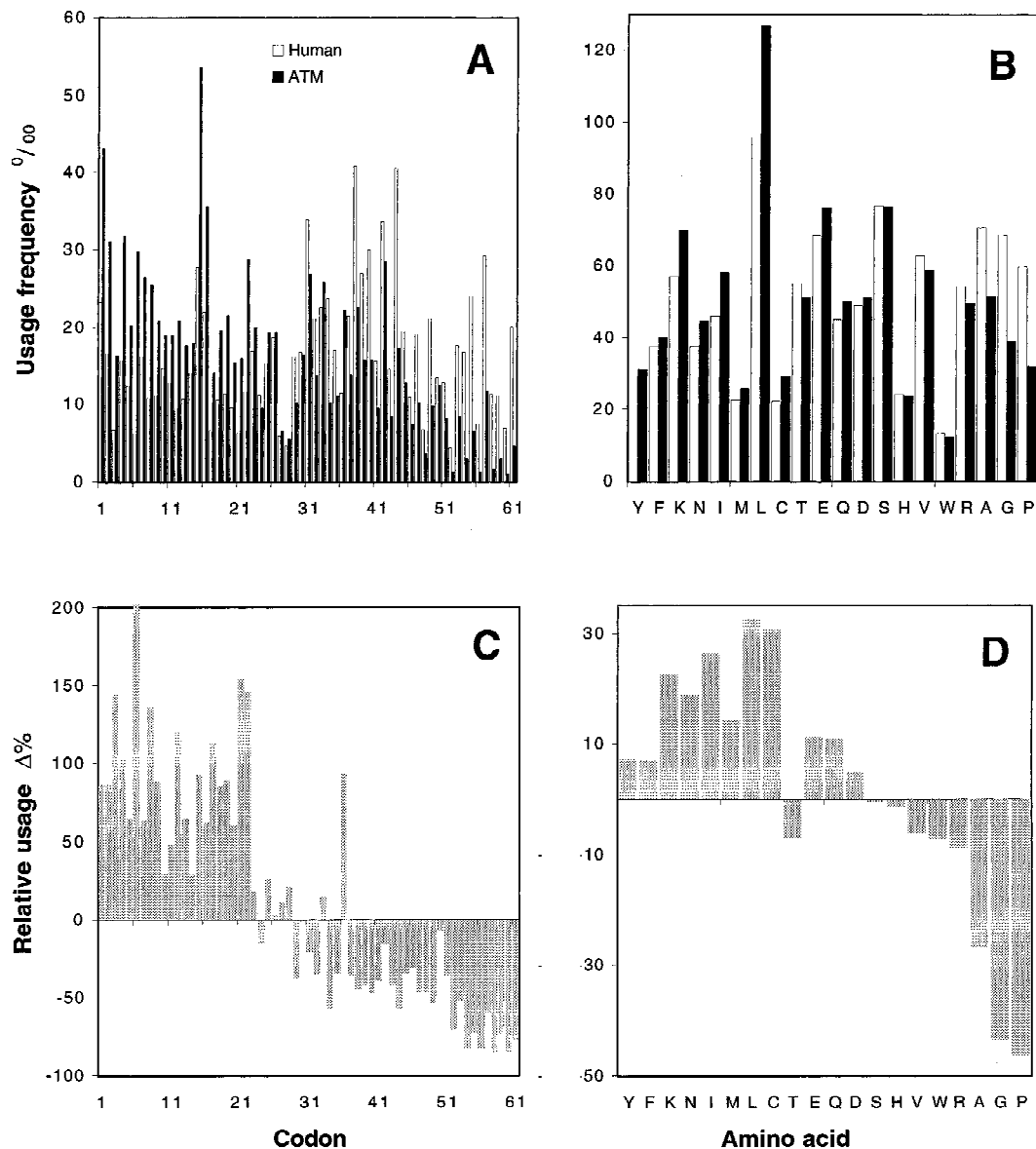


Figure 6 Absolute and relative usage of codons (A,C) and amino acids (B,D) of the *ATM* gene in comparison with the human average. Codons are ordered from *left to right* with primary sort criterion “3rd codon position A or T” and secondary criterion “increasing G + C content.” The order of columns is (1) AAA; (2) AAT; (3) ATA; (4) ATT; (5) TAT; (6) TTA; (7) TTT; (8) AGA; (9) AGT; (10) ACA; (11) ACT; (12) TGT; (13) TCA; (14) TCT; (15) GAA; (16) GAT; (17) GTA; (18) GTT; (19) CAA; (20) CAT; (21) CTA; (22) CTT; (23) GGA; (24) GGT; (25) GCA; (26) GCT; (27) CGA; (28) CGT; (29) CCA; (30) CCT; (31) AAG; (32) AAC; (33) ATG; (34) ATC; (35) TAC; (36) TTG; (37) TTC; (38) GAG; (39) GAC; (40) GTG; (41) GTC; (42) CAG; (43) CAC; (44) CTG; (45) CTC; (46) AGG; (47) AGC; (48) ACG; (49) ACC; (50) TGG; (51) TGC; (52) TCG; (53) TCC; (54) GGG; (55) GGC; (56) GCG; (57) GCC; (58) CGG; (59) CGC; (60) CCG; (61) CCC. Amino acids are tentatively arranged from *left to right* order of increasing G + C content of their codons. Columns are labeled with the single letter code.

located in an A + T-rich isochores, for which a very low gene density is expected (Mouchiroud et al. 1991). Their proximity raises the possibility of coordinate gene expression. In humans, ~60% of genes are associated with CpG islands, including all

housekeeping genes analyzed so far (Antequera and Bird 1993). The ubiquitous expression of both the *ATM* and *E14/NPAT* genes in all tissues examined to date (Savitsky et al. 1995a; Byrd et al. 1996b; Imai 1996) is consistent with the definition of house-

Table 4. Potential Promoter Elements Predicted by TSSG, TSSW, and PSII Algorithms

No. ^a	Score	TSSG TATA	Start	Score	TSSW TATA	Start	Score	PSII TATA	Start
F1	13.3	714	743	—	—	—			
R1	8.1	10,359	10,342	8.7	—	10,393			
F2	7.0	—	10,513	9.9	—	10,513			
F3	6.7	14,699	14,739	9.3	14,699	14,739			
R2	16.9	74,575	74,546	—	—	—	60.5	75,512	75,542
F4									
F3	15.1	80,433	80,404	—	—	—			
F5	13.4	—	90,302	—	—	—			
R4							73.7	115,070	115,040
F6	9.7	132,369	132,399	9.8	132,369	132,399			
F7							59.9	141,310	141,340
F8	10.0	144,768	144,810	—	—	—			
R5	7.5	176,805	176,775	9.8	176,805	176,773			

To limit the output of these programs to high-score predictions, the cutoff values were adjusted to 8, 9, and 55. Predictions with lower score values were reported only when the score value of this element exceeded the respective cutoff score in one of the other programs.

^a(F) Promoter oriented forward with respect to *ATM* transcription; (R) reverse orientation.

keeping genes. Reporter gene constructs showed that the CpG island functions as a bidirectional promoter and that expression directed toward *ATM* was threefold higher than toward *E14/NPAT* (Byrd et al. 1996b). In agreement with these studies, 20 hits were found in the public EST databases for *ATM*, whereas only three were found for *E14/NPAT*. The majority of the *ATM*-specific ESTs map to the 3' UTR and only one clone matches the coding region. In the case of *E14/NPAT*, all three ESTs map to the coding region. This highlights the fact that public ESTs databases are strongly biased toward the 3' end of mRNA. For this reason, coding regions of genes with very long 3' UTRs, like that of the *ATM* gene are significantly underrepresented.

The transcripts of the *ATM* gene belong to the 5%–10% of vertebrate mRNAs that have long, highly structured 5' UTRs (Savitsky et al. 1997). These genes often use alternative promoters to generate supplementary transcripts with short leader sequences (Kozak 1992; Ayoubi and Van De Ven 1996). Interestingly, an additional putative *ATM* promoter, containing a TATA-box, was found within intron 3, immediately upstream of the first coding exon. No transcripts have yet been found that are driven by this promoter, although some of the short bands observed by primer extension might be transcribed from from this promoter (K. Savitsky, unpubl.). Remarkably, the promoter predicted in intron 3 depends on several elements re-

siding within two *Alu* repeats. Previously, most *Alu* sequences have been considered functionally inert. However, recent studies provide strong evidence that significant subsets of *Alu* repeats can confer hormone responsiveness to a promoter. Two members of different *Alu* classes (Sp and Sc) can function as estrogen receptor-dependent transcriptional enhancers (Norris et al. 1995). A unique point mutation in an ERE-like sequence motif (G to A at position 93 of the *Alu* consensus; Batzer et al. 1996) activates the enhancer. We have found a similar G to A base change in an *Alu* repeat of *ATM* intron 3 just downstream of the predicted promoter. This element is therefore identical to the proposed consensus of the *Alu* ERE except that the half-site (5'-TGACC-3') is located 7 bp instead of 9 bp downstream from the imperfect ERE (5'-GGTCAnnnTG-GTC-3'). The existence of several putative promoter regions containing multiple regulatory motifs, and the extensive structural diversity of the 5' and 3' UTRs suggest complex posttranscriptional regulation of the *ATM* gene. In this respect, the putative promoter within intron 3 could supply the short 5'UTR that will allow the basal levels of *ATM* translation, whereas the different 5'UTRs coming from the upstream promoter, would supply regulative UTRs (Savitsky et al. 1997).

In summary, the presented 184,490 bp of genomic sequence containing the human *ATM* gene provides a substantial resource for further investiga-

PLATZER ET AL.

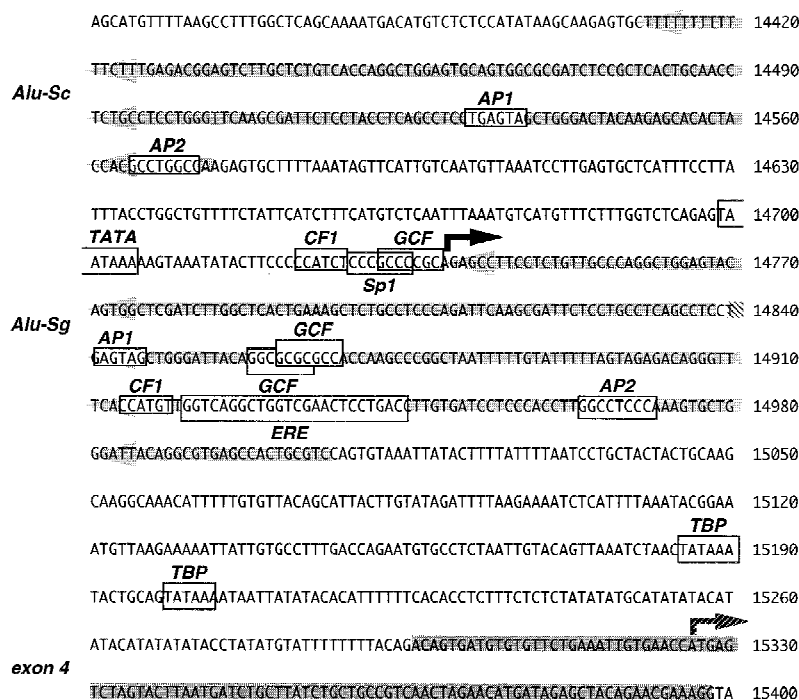


Figure 7 Nucleotide sequence of the putative promoter located in intron 3. The darkly shaded region indicates exon 4, lightly shaded arrows the two *Alu* repeats. Potential binding sites for transcription factors are boxed. The predicted transcription start site is marked by a bold arrow; the *ATM* start codon by a hatched arrow. Numbers along the right side of the figure indicate the nucleotide numbering of the database entry (accession no. U82828).

tion of *ATM* regulation, for the detection of mutations and polymorphisms in this gene, and for the development of diagnostic tools. The analysis of the region demonstrates the capability of ongoing large-scale sequencing efforts in addressing questions of organization and evolution in human genes and chromosome regions. Comparative sequencing in model organisms will provide further insights into these processes.

METHODS

Cosmids

A chromosome 11-specific cosmid library, cloned in the vector sCos1, was a gift from Dr. Larry Deaven (Los Alamos National Laboratory, NM). High-density arrayed grids from this library were screened using yeast artificial chromosome (YAC) clones y67 and y41 (Rotman et al. 1994). YAC probes were prepared by fragmenting 20 ng of YAC DNA for 20 min at 100°C, and subsequent labeling by random oligo priming using [α - 32 P]dCTP. To prevent nonspecific hybridization, YAC probes were blocked by incubation with 30 μ g Cot-1 DNA (GIBCO BRL), 3 mg of total human placenta DNA (Sigma),

and 4 μ g of vector sCos-1 DNA, at 100°C for 10 min in a final volume of 1 ml. NaPO_4 (pH 7.2), was added to a final concentration of 120 mM, and the mixture was incubated further at 65°C for 3 hr, before its addition at 1×10^6 cpm/ml to the final hybridization solution (0.25 M NaPO_4 at pH 7.2, 0.25 M NaCl, 5% SDS, 10% PEG-8000, 1 mM EDTA). Filters were rinsed in $0.2 \times \text{SSC}$, 0.5% SDS at 60°C for 10 to 15 min, and exposed to X-ray film for 24 hr.

Positive clones were aligned by identifying overlaps between them. DNA blots containing cosmid DNA digested with *TaqI* and *HindIII* were hybridized with genetic markers, total cosmid inserts, YACs and cosmid ends, or moderately repetitive elements. Common hybridizing bands for any two cosmids were defined as overlaps.

Sequencing

The cosmids were prepared and sequenced as described previously (Craxton 1993) with several modifications. M13 templates were prepared by the triton method (Mardis 1994) and sequenced using Thermo Sequenase (Amersham). In the shotgun phase of a cosmid sequencing project, identical amounts of samples were sequenced either by dye-primer or dye-terminator chemistries (Perkin Elmer). Data were collected using ABI 373 and 377 automated sequencers and assembled with the XGAP program (Dear and Staden 1991). Gaps were closed using custom-made primers on M13 templates, PCR products, or cosmid DNA in combination with dye terminators. Regions of the final assembly that only consist of dye-

primer reads were resequenced using dye-terminator chemistry to resolve all compressions.

Standard PCR conditions for amplification of selected regions of genomic DNA were: 1 min at 94°C, 30 cycles (30 sec at 94°C, 1 min at 55°C, 2 min at 72°C), 4 min at 72°C. Introns 24–26 were amplified using the Expand Long Template PCR System (Boehringer Mannheim) and primer pairs gctgatcctattcaaatggg and ctctcattectctgagcttc, gttccaggacagaaggag and cacaaggtgaggttctaatec, and ccatagtgtgagaacctg and tagaaatcctcaatattgtgtag, respectively. PCR products appearing as a single clean and distinct band on agarose gels were purified by PEG precipitation (Rosenthal et al. 1993). Otherwise, the appropriate bands were cut out of the agarose gel and purified using the Qiaex Kit (Qiagen). Sequencing was performed using the PCR primers or internal primers using dye-terminator chemistry (Perkin Elmer). Five micrograms of intron 24-specific PCR product were used to prepare a M13 shotgun library that was sequenced as described above.

Computer Analysis

Homology searches against the EMBL database were performed using BLAST (version 1.4) (Altschul et al. 1990) and FASTA (version 2.0) (Pearson and Lipman 1988). Programs XGAP (Uberbacher and Mural 1991) and XPOUND (Thomas and Skolnick 1994) were used for exon prediction. Ge-

SEQUENCE ANALYSIS OF HUMAN ATM

nome-wide repeats were identified using the CENSOR program (Jurka et al. 1996). Local base content was determined with the LPC algorithm (Huang 1994a). The Wisconsin Sequence Analysis Package (Genetics Computer Group, Inc.) was used to determine G + C%, G + C distribution, and codon usage. The window for calculation of the G + C distribution was set at ± 2 kb for global and at ± 0.2 kb for local analysis and moved in steps of 1 and 0.1 kb, respectively. Statistical analysis was performed by Excel 5.0 (Microsoft Corp.). The identification of CpG islands (V.G. Micklem, pers. comm.) was achieved using the following criteria: G + C > 50%, CpG ratio observed/expected > 0.6, length > 200 bp (Gardiner and Frommer 1987). Sequence alignments were performed using the Global Alignment Program (GAP) (Huang 1994b). To evaluate the significance of sequence similarities we used PRDF (W.R. Pearson, pers. comm.). The human codon usage table was obtained from the Codon Usage Database (Nakamura et al. 1996) compiled from GenBank release 96. Several computer programs were applied for promoter prediction: (1) "Transcription Start Site" using both Ghosh/Prestridge (TSSG) motif data and Wingender (TSSW) motif database (<http://dot.imgen.bcm.tmc.edu:9331/gen-e-finder/help/tssw.html>); (2) "Promoter Scan II" (PSII; Prestridge 1995); (3) Neural Network Promoter Prediction (NNPP; <http://www-hgc.lbl.gov/projects/promoter.html>); (4) Signal Scan (SS; Prestridge 1991); and (5) Transcription Factor Search 1.3 (TFS; <http://www.genome.ad.jp/htbin/nph-tfsearch>).

ACKNOWLEDGMENTS

We thank Diana Wiedemann and Hella Ludewig for the excellent technical assistance.

The publication costs of this article were defrayed in part by payment of page charges. This article must therefore be hereby marked "advertisement" in accordance with 18 USC section 1734 solely to indicate this fact.

REFERENCES

- Aebi, M., H. Hornig, and C. Weissmann. 1987. 5' cleavage site in eukaryotic pre-mRNA splicing is determined by the overall 5' splice region, not by the conserved 5' GU. *Cell* **50**: 237–246.
- Altschul, S.F., W. Gish, W. Miller, E.W. Myers, and D.J. Lipman. 1990. Basic local alignment search tool. *J. Mol. Biol.* **215**: 403–410.
- Ambrose, H.J., P.J. Byrd, C.M. McConville, P.R. Cooper, T. Stankovic, J.H. Riley, Y. Shiloh, J.O. McNamara, T. Fukao, and A.M. Taylor. 1994. A physical map across chromosome 11q22-q23 containing the major locus for ataxia telangiectasia. *Genomics* **21**: 612–619.
- Antequera, F. and A. Bird. 1993. Number of CpG islands and genes in human and mouse. *Proc. Natl. Acad. Sci.* **90**: 11995–11999.
- Ayoubi, T.A. and W.J. Van De Ven. 1996. Regulation of gene expression by alternative promoters. *FASEB J.* **10**: 453–460.
- Batzer, M.A., S.S. Arcot, J.W. Phinney, M. Alegria-Hartman, D.H. Kass, S.M. Milligan, C. Kimpton, P. Gill, M. Hochmeister, P.A. Ioannou, R.J. Herrera, D.A. Boudreau, W.D. Scheer, B.J. Keats, P.L. Deininger, and M. Stoneking. 1996. Genetic variation of recent Alu insertions in human populations. *J. Mol. Evol.* **42**: 22–29.
- Baumer, A., U. Bernthaler, W. Wolz, H. Hoehn, and D. Schindler. 1996. New mutations in the ataxia telangiectasia gene. *Hum. Genet.* **98**: 246–249.
- Bernardi, G. 1995. The human genome: Organization and evolutionary history. *Annu. Rev. Genet.* **29**: 445–476.
- Bernardi, G., B. Olofsson, J. Filipski, M. Zerial, J. Salinas, G. Cuny, M. Meunier-Rotival, and F. Rodier. 1985. The mosaic genome of warm-blooded vertebrates. *Science* **228**: 953–958.
- Bollag, R.J., A.S. Waldman, and R.M. Liskay. 1989. Homologous recombination in mammalian cells. *Annu. Rev. Genet.* **23**: 199–225.
- Broom, J.E., D.F. Hill, G. Hughes, W.A. Jones, J.C. McNaughton, P.A. Stockwell, and G.B. Petersen. 1995. Sequence of a transposon identified as Tn1000 (gamma delta). *DNA Seq.* **5**: 185–189.
- Byrd, P.J., C.M. McConville, P. Cooper, J. Parkhill, T. Stankovic, G.M. McGuire, J.A. Thick, and A.M. Taylor. 1996a. Mutations revealed by sequencing the 5' half of the gene for ataxia telangiectasia. *Hum. Mol. Genet.* **5**: 145–149.
- Byrd, P.J., P.R. Cooper, T. Stankovic, H.S. Kullar, G.D. Watts, P.J. Robinson, and M.R. Taylor. 1996b. A gene transcribed from the bidirectional ATM promoter coding for a serine rich protein: Amino acid sequence, structure and expression studies. *Hum. Mol. Genet.* **5**: 1785–1791.
- Chen, E.Y., M. Zollo, R. Mazarrella, A. Ciccodicola, C. Chen, L. Zuo, C. Heiner, F. Burrough, M. Repetto, D. Schlessinger, and M. D'Urso. 1996. Long-range sequence analysis in Xq28: Thirteen known and six candidate genes in 219.4 kb of high GC DNA between the RCP/GCP and G6PD loci. *Hum. Mol. Genet.* **5**: 659–668.
- Craxton, M. 1993. Cosmid sequencing. *Methods Mol. Biol.* **23**: 149–167.
- Cross, S.H. and A.P. Bird. 1995. CpG islands and genes. *Curr. Opin. Genet. Dev.* **5**: 309–314.
- Cross, S.H., J.A. Charlton, X. Nan, and A.P. Bird. 1994. Purification of CpG islands using a methylated DNA binding column. *Nature Genet.* **6**: 236–244.
- Dear, S. and R. Staden. 1991. A sequence assembly and editing program for efficient management of large projects. *Nucleic Acids Res.* **19**: 3907–3911.
- Dombroski, B.A., S.L. Mathias, E. Nanthakumar, A.F. Scott, and H.H. Kazazian, Jr. 1991. Isolation of an active human transposable element. *Science* **254**: 1805–1808.
- Duret, L., D. Mouchiroud, and C. Gautier. 1995. Statistical analysis of vertebrate sequences reveals that long genes are scarce in GC-rich isochores. *J. Mol. Evol.* **40**: 308–317.

PLATZER ET AL.

- Fukagawa, T., K. Sugaya, K. Matsumoto, K. Okumura, A. Ando, H. Inoko, and T. Ikemura. 1995. A boundary of long-range G + C% mosaic domains in the human MHC locus: Pseudoautosomal boundary-like sequence exists near the boundary. *Genomics* **25**: 184–191.
- Gardiner-Garden, M. and M. Frommer. 1987. CpG islands in vertebrate genomes. *J. Mol. Biol.* **196**: 261–282.
- Gatti, R.A., I. Berkel, E. Boder, G. Braedt, P. Charmley, P. Concannon, F. Ersoy, T. Foroud, N.G. Jaspers, K. Lange et al. 1988. Localization of an ataxia-telangiectasia gene to chromosome 11q22-23. *Nature* **336**: 577–580.
- Gilad, S., R. Khosravi, D. Shkedy, T. Uziel, Y. Ziv, K. Savitsky, G. Rotman, S. Smith, L. Chessa, T.J. Jorgensen, R. Harnik, M. Frydman, O. Sanal, S. Portnoi, Z. Goldwicz, N.G. Jaspers, R.A. Gatti, G. Lenoir, M.F. Lavin, K. Tatsumi, R.D. Wegner, Y. Shiloh, and A. Bar-Shira. 1996. Predominance of null mutations in ataxia-telangiectasia. *Hum. Mol. Genet.* **5**: 433–439.
- Holmquist, G.P. 1992. Chromosome bands, their chromatin flavors, and their functional features. *Am. J. Hum. Genet.* **51**: 17–37.
- Huang, X. 1994a. An algorithm for identifying regions of a DNA sequence that satisfy a content requirement. *Comput. Appl. Biosci.* **10**: 219–225.
- . 1994b. On global sequence alignment. *Comput. Appl. Biosci.* **10**: 227–235.
- Ikemura, T., K. Wada, and S. Aota. 1990. Giant G + C% mosaic structures of the human genome found by arrangement of GenBank human DNA sequences according to genetic positions. *Genomics* **8**: 207–216.
- Imai, T., M. Yamauchi, N. Seki, T. Sugawara, T. Saito, Y. Matsuda, H. Ito, T. Nagase, N. Nomura, and T. Hori. 1996. Identification and characterization of a new gene physically linked to the ATM gene. *Genome Res.* **6**: 439–447.
- Jackson, I.J. 1991. A reappraisal of non-consensus mRNA splice sites. *Nucleic Acids Res.* **19**: 3795–3798.
- Jurka, J., P. Klonowski, V. Dagman, and P. Pelton. 1996. CENSOR—a program for identification and elimination of repetitive elements from DNA sequences. *Comput. Chem.* **20**: 119–121.
- Kozak, M. 1992. Regulation of translation in eukaryotic systems. *Annu. Rev. Cell Biol.* **8**: 197–225.
- Lavin, M.F. and Y. Shiloh. 1997. The genetic defect in ataxia-telangiectasia. *Annu. Rev. Immunol.* **15**: 177–222.
- Lopez, R., F. Larsen, and H. Prydz. 1994. Evaluation of the exon predictions of the GRAIL software. *Genomics* **24**: 133–136.
- Mardis, E.R. 1994. High-throughput detergent extraction of M13 subclones for fluorescent DNA sequencing. *Nucleic Acids Res.* **22**: 2173–2175.
- Mouchiroud, D., G. D’Onofrio, B. Aissani, G. Macaya, C. Gautier, and G. Bernardi. 1991. The distribution of genes in the human genome. *Gene* **100**: 181–187.
- Nakamura, Y., K. Wada, Y. Wada, H. Doi, S. Kanaya, T. Gojobori, and T. Ikemura. 1996. Condon usage tabulated from the international DNA sequence databases. *Nucleic Acids Res.* **24**: 214–215.
- Norris, J., D. Fan, C. Aleman, J.R. Marks, P.A. Futreal, R.W. Wiseman, J.D. Iglehart, P.L. Deininger, and D.P. McDonnell. 1995. Identification of a new subclass of Alu DNA repeats which can function as estrogen receptor-dependent transcriptional enhancers. *J. Biol. Chem.* **270**: 22777–22782.
- Pearson, W.R. and D.J. Lipman. 1988. Improved tools for biological sequence comparison. *Proc. Natl. Acad. Sci.* **85**: 2444–2448.
- Prestridge, D.S. 1991. SIGNAL SCAN: A computer program that scans DNA sequences for eukaryotic transcriptional elements. *Comput. Appl. Biosci.* **7**: 203–206.
- . 1995. Predicting Pol II promoter sequences using transcription factor binding sites. *J. Mol. Biol.* **249**: 923–932.
- Rasio, D., S.A. Schichman, M. Negrini, E. Canaani, and C.M. Croce. 1996. Complete exon structure of the ALL1 gene. *Cancer Res.* **56**: 1766–1769.
- Roberts, R.G., A.J. Coffey, M. Bobrow, and D.R. Bentley. 1993. Exon structure of the human dystrophin gene. *Genomics* **16**: 536–538.
- Rosenthal, A., O. Coutelle, and M. Craxton. 1993. Large-scale production of DNA sequencing templates by microtitre format PCR. *Nucleic Acids Res.* **21**: 173–174.
- Rotman, G., K. Savitsky, Y. Ziv, C.G. Cole, M.J. Higgins, I. Bar-Am, I. Dunham, A. Bar-Shira, L. Vanagaite, and S. Qin. 1994. A YAC contig spanning the ataxia-telangiectasia locus (groups A and C) at 11q22-q23. *Genomics* **24**: 234–242.
- Savitsky, K., A. Bar-Shira, S. Gilad, G. Rotman, Y. Ziv, L. Vanagaite, D.A. Tagle, S. Smith, T. Uziel, S. Sfez, et al. 1995a. A single ataxia telangiectasia gene with a product similar to PI-3 kinase. *Science* **268**: 1749–1753.
- Savitsky, K., S. Sfez, D.A. Tagle, Y. Ziv, A. Sartieli, F.S. Collins, Y. Shiloh, and G. Rotman. 1995b. The complete sequence of the coding region of the ATM gene reveals similarity to cell cycle regulators in different species. *Hum. Mol. Genet.* **4**: 2025–2032.
- Savitsky, K., M. Platzer, T. Uziel, S. Gilad, A. Sartieli, A. Rosenthal, O. Elroy-Stein, Y. Shiloh, and G. Rotman. 1997. Ataxia-telangiectasia: Structural diversity of untranslated sequences suggests complex posttranscriptional regulation of the ATM gene expression. *Nucleic Acids Res.* **25**: 1678–1684.
- Shapiro, M.B. and P. Senapathy. 1987. RNA splice junctions of different classes of eukaryotes: Sequence statistics and

SEQUENCE ANALYSIS OF HUMAN ATM

functional implications in gene expression. *Nucleic Acids Res.* **15**: 7155–7174.

Shiloh, Y. 1995. Ataxia-telangiectasia: Closer to unraveling the mystery. *Eur. J. Hum. Genet.* **3**: 116–138.

Smit, A.F. 1993. Identification of a new, abundant superfamily of mammalian LTR-transposons. *Nucleic Acids Res.* **21**: 1863–1872.

Smit, A.F. and A.D. Riggs. 1995. MIRs are classic, tRNA-derived SINEs that amplified before the mammalian radiation. *Nucleic Acids Res.* **23**: 98–102.

———. 1996. Tiggers and DNA transposon fossils in the human genome. *Proc. Natl. Acad. Sci.* **93**: 1443–1448.

Smit, A.F., G. Toth, A.D. Riggs, and J. Jurka. 1995. Ancestral, mammalian-wide subfamilies of LINE-1 repetitive sequences. *J. Mol. Biol.* **246**: 401–417.

Swift, M., D. Morrell, R.B. Massey, and C.L. Chase. 1991. Incidence of cancer in 161 families affected by ataxia-telangiectasia [see comments]. *N. Engl. J. Med.* **325**: 1831–1836.

Telatar, M., Z. Wang, N. Udar, T. Liang, E. Bernatowska-Matuszkiewicz, M. Lavin, Y. Shiloh, P. Concannon, R.A. Good, and R.A. Gatti. 1996. Ataxia-telangiectasia: Mutations in ATM cDNA detected by protein-truncation screening. *Am. J. Hum. Genet.* **59**: 40–44.

Thomas, A. and M.H. Skolnick. 1994. A probabilistic model for detecting coding regions in DNA sequences. *IMA. J. Math. Appl. Med. Biol.* **11**: 149–160.

Uberbacher, E.C. and R.J. Mural. 1991. Locating protein-coding regions in human DNA sequences by a multiple sensor-neural network approach. *Proc. Natl. Acad. Sci.* **88**: 11261–11265.

Uziel, T., K. Savitsky, M. Platzer, Y. Ziv, T. Helbitz, M. Nehls, T. Boehm, A. Rosenthal, Y. Shiloh, and G. Rotman. 1996. Genomic Organization of the ATM gene. *Genomics* **33**: 317–320.

Vorechovsky, I., D. Rasio, L. Luo, C. Monaco, L. Hammarstrom, A.D. Webster, J. Zaloudik, G. Barbanti-Brodani, M. James, G. Russo, C.M. Croce, and M. Negrini. 1996. The ATM gene and susceptibility to breast cancer: analysis of 38 breast tumors reveals no evidence for mutation. *Cancer Res.* **56**: 2726–2732.

Weeks, D.E., M.C. Paterson, K. Lange, B. Andrais, R.C. Davis, F. Yoder, and R.A. Gatti. 1991. Assessment of chronic gamma radiosensitivity as an in vitro assay for heterozygote identification of ataxia-telangiectasia. *Radiat. Res.* **128**: 90–99.

Wright, J., S. Teraoka, S. Onengut, A. Tolun, R.A. Gatti, H.D. Ochs, and P. Concannon. 1996. A high frequency of distinct ATM gene mutations in ataxia-telangiectasia. *Am. J. Hum. Genet.* **59**: 839–846.

Yang, Z., M. Sugawara, P.D. Ponath, L. Wessendorf, J. Banerji, Y. Li, and J.L. Strominger. 1990. Interferon gamma response region in the promoter of the human DPA gene. *Proc. Natl. Acad. Sci.* **87**: 9226–9230.

Zakian, V.A. 1995. ATM-related genes: What do they tell us about functions of the human gene? *Cell* **82**: 685–687.

Received February 19, 1997; accepted in revised form April 15, 1997.



Ataxia-Telangiectasia Locus: Sequence Analysis of 184 kb of Human Genomic DNA Containing the Entire *ATM* Gene

Matthias Platzer, Galit Rotman, David Bauer, et al.

Genome Res. 1997 7: 592-605

Access the most recent version at doi:[10.1101/gr.7.6.592](https://doi.org/10.1101/gr.7.6.592)

References This article cites 64 articles, 12 of which can be accessed free at:
<http://genome.cshlp.org/content/7/6/592.full.html#ref-list-1>

License

Email Alerting Service Receive free email alerts when new articles cite this article - sign up in the box at the top right corner of the article or [click here](#).

Affordable, Accurate
Sequencing.



To subscribe to *Genome Research* go to:
<https://genome.cshlp.org/subscriptions>
